Further Comparisons of Interactive Boundary-Layer and Thin-Layer Navier-Stokes Procedures

K. C. Chang*
Douglas Aircraft Company, Long Beach, California

N. Alemdaroglu†
California State University, Long Beach, California

Unmeel Mehta‡
NASA Ames Research Center, Moffett Field, California

and

Tuncer Cebeci§
Douglas Aircraft Company, Long Beach, California

Calculations of the flows over NACA 4412 and GA(W)-2 airfoils with low-speed flow and over NACA 0012 and RAE 2822 airfoils with transonic flow are reported. They were obtained by solving potential flow and boundary-layer equations, and by solving thin-layer Navier-Stokes equations. The results cover a range of angles of attack up to and including stall and allow the evaluation of the numerical and physical features of the two solution methods. The agreement with measurements is acceptable except between the results of the thin Navier-Stokes equations and measurements in subsonic flow at high angles of attack. The interactive boundary-layer method is considerably more efficient, requiring considerably less computer time and storage.

Introduction

THE calculated results presented here allow detailed comparison of procedures based on two reduced forms of the Navier-Stokes equations. They supplement the previous work of Ref. 1, which was concerned with low-speed flow over a NACA 0012 airfoil, and include consideration of two airfoils with low-speed flow and two with transonic flow. The comparison of the two procedures with each other is concerned with their efficiency and numerical accuracy; the comparisons with experiment permit assessment of their ability to represent a range of flows.

The time-averaged thin-layer Navier-Stokes (TLNS) equations are a reduced form of general equations with neglected longitudinal diffusion and are considered here in two-dimensional form. The time-averaged two-dimensional boundary-layer equations are formulated with the same assumptions and with the neglect of convection, diffusion, and pressure gradient normal to the direction of preferred flow. The boundary-layer equations are, however, solved together with the inviscid-flow equations that do represent normal convection outside the boundary layer so that the relative advantages of numerical methods based on the two equation forms cannot be quantified a priori. The calculations of Ref. 1 have shown that both forms can result in accurate values of lift coefficient up to moderate angles of attack. The interactive boundary-layer (IBL) approach is preferable at high angles of attack and also provides better representation of lift. The total drag coefficients computed by both procedures agree with each other at small angles of attack, but those computed by IBL deviate from those computed by TLNS at higher angles of attack. It is also evident that the added cost associated with the use of the TLNS approach can be considerable.

Since the equations are solved in time-averaged form, a turbulence model is required and an eddy-viscosity hypothesis is employed with both approaches. As in Ref. 1, the algebraic formulation of Ref. 2 is used in the IBL method. A modified form of this model[3] is used with the TLNS equations. The interactive method, again, makes use of a conformal mapping procedure to solve the potential-flow equations[4] for low-speed flow. The transonic-flow calculations made use of the full potential approach of Bauer et al.[5] with modifications as described in Ref. 6. It is not expected that the method used to solve the inviscid-flow equations influences the conclusions. The different turbulence models of the two approaches are also likely to have a small influence[7] except in the wake region where the turbulence model of the IBL procedure[8] is different from that used in the TLNS procedure.

The paper has been prepared with four further sections that are concerned with describing the IBL and TLNS methods, results and discussion, and summary conclusions. The descriptions in the sections are brief, since more detailed descriptions are available in Refs. 1, 9–11 for subsonic flow, and in Ref. 12 for transonic flow.

Interactive Boundary-Layer Procedure

This procedure involves the solution of inviscid- and viscous-flow equations, the latter in inverse form, and the Hilbert integral approach[11] to link the two sets of equations through a blowing velocity. Two methods were used to solve the inviscid-flow equations, one for subsonic and the other for transonic flow. The method of Refs. 5 and 6 could have been used for both types of flow, but that of Ref. 4 was preferred for subsonic flows since this method has a number of very desirable features.[10] The following subsections describe the two inviscid-flow methods and the interactive boundary-layer method.

Received Dec. 10, 1986; presented as Paper 87-0430 at the AIAA 25th Aerospace Sciences Meeting, Reno, NV, Jan. 12–15, 1987; revision received Nov. 24, 1987.

*Senior Engineer/Scientist, Aerodynamic Research and Technology Group. Associate Fellow AIAA.

†Associate Professor, Center for Aerodynamics Research. Member AIAA.

‡Research Scientist, Computational Fluid Dynamics Branch. Associate Fellow AIAA.

§Staff Director, Aerodynamic Research and Technology Group. Fellow AIAA.

Inviscid Flow: Subsonic Flow

The conformal-mapping approach of Halsey[4] involves transformation of the region outside the airfoil to that outside a unit circle and the solution of the inviscid-flow equations within this transformed plane. It makes use of Fourier analysis techniques to expand the complex velocity to an infinite series involving a constant and negative powers of the complex coordinate. The major computational effort is in the transformation, which needs to be performed only once so that the approach is efficient.

The influence of the inviscid flow on the wake is simulated by a distribution of sources and sinks along the inviscid trailing streamline and its reflection in the unit circle. At high angles of attack, care is required to deal with displacement thicknesses of up to 10% chord in the region close to the trailing edge. The blowing velocity is calculated at the displacement surface and applied on the airfoil surface to avoid difficulties associated with the near-wall pressure gradient. The Kutta condition is modified to apply the displacement surface, on the locations of the velocity values, with the assumption equal off-body pressure at the upper and lower trailing-edge points. Further details are provided in Ref. 10.

Inviscid Flow: Transonic Flow

In the method of Refs. 5 and 6, conformal mapping is again used with the inviscid equations solved in the transformed plane by a successive line over-relaxation method combined with a fast elliptic solver which provides rapid convergence of the solution in the subsonic region, while the over-relaxation ensures convergence in the supersonic flow regions. An artificial viscosity term is introduced to allow the degree of conservation of the finite-difference scheme to be selected at any level between conservative and nonconservative.

The initial inviscid velocity iterations make use of a Kutta condition that ensures finite velocity at the trailing edge by introducing a stagnation point at the corresponding point in the computational plane. As the boundary-layer calculations are performed, a blowing velocity is again introduced on the airfoil surface to simulate the viscous effects. In addition, the Kutta condition is modified to ensure that velocity magnitudes at the edge of the displacement thickness match at the trailing edge, and this is accomplished by interpolation. The procedure also accounts for the effects of the viscous wake by applying wake boundary conditions along the grid line through the trailing edge so that the shape of the wake is independent of the angle of attack. This limitation is not serious, since the boundary condition applied on the wake takes the form of a specified normal velocity jump, which rapidly decreases away from the trailing edge.

Interactive Boundary Layer

The boundary-layer equations for steady, two-dimensional, external flow are well known and are solved here with eddy-viscosity and turbulent Prandtl-number assumptions. The algebraic eddy-viscosity formulation of Cebeci and Smith[2] as described in Ref. 10 is preferred because it provides the best compromise between accuracy and simplicity, and a constant value of 0.9 is assumed for the turbulent Prandtl number. The equations representing conservation of mass, momentum, and energy are solved with Keller's box method, which is an efficient and accurate second-order finite-difference method used by Cebeci and associates for a wide range of flows.[13]

Interaction between the inviscid and viscous flows is achieved by a blowing-velocity distribution that is linked to the displacement-thickness distribution through the Hilbert integral. Where separation is encountered, the equations are solved in inverse form with the FLARE approximation that neglects longitudinal convection in the recirculating region. The same approach is taken in the wake where the dividing streamline is computed from the conformal mapping procedure as a line having constant stream function. It is also used by the inviscid method to apply the blowing velocity required to simulate the displacement thickness and to compute the inviscid velocity. An inviscid point distribution in the wake is defined where the wake blowing velocity is defined, and where the wake velocity distribution is determined. This requires interpolation of the boundary-layer blowing velocity to the inviscid points. In addition, the computed inviscid velocity is interpolated back to the boundary-layer points by making use of the computed velocity at the trailing edge as the initial wake point. In the immediate vicinity of the trailing edge, particular care is required in the choice of locations at which values of the blowing velocities are applied in the solution of the inviscid equations. The use of the FLARE approximation in wakes with separation upstream of the trailing edge (as compared to wall boundary layers where the separated region is close to the wall) can pose numerical difficulties. As in Ref. 10, however, the continuation method was used to overcome the problem.

Thin-Layer Navier-Stokes Procedure

The thin-layer equations are generally referred to in the literature as TLNS equations. They are obtained by neglecting streamwise and spanwise derivatives of the viscous and turbulence stress, conductive heat-flux terms, and any term involving mixed derivatives. (For a detailed discussion, see Refs. 14 and 15.) These approximations are justified either by order of magnitude arguments or by consideration of the computational accuracy argument. The TLNS equations have been proposed mainly on the computational argument. The form of the equations generally used does not satisfy relationships between metric coefficients in diffusive and conduction terms, but the resulting error is usually insignificant, except when the effective viscosity is relatively large. In addition, longitudinal-curvature diffusive terms are neglected as a consequence of the Cartesian velocity components.

An implicit numerical method is used to solve the TLNS equations and is based on that of Ref. 16. Since only steady-state computations are of interest, a diagonal form for the Euler equations and a spatially varying time step are used. Reference 9 provides a description of the numerical scheme to obtain the results presented here. The turbulence model incorporated in the code is described in Ref. 1.

Results

Measurements of the flow around a NACA 4412 airfoil have been reported in Refs. 17 and 18 and made use of flying hot-wire anemometry to obtain results at angles of attack up to that of maximum lift. The Reynolds number based on chord length was 1.523×10^6 and transition was induced at 2.5% chord on the upper surface and 10.3% chord on the lower surface. The same Reynolds number and transition locations were used in the calculations with both methods at angles of attack up to 12 deg. Above 12 deg, the interactive calculations revealed a laminar separation very close to the leading edge, and the location of the onset of this separation was taken as that of the onset of transition. This assumption is consistent with transition having occurred upstream of the trip in the experiment.

The flow around a NACA 4412 airfoil has also been investigated at a chord Reynolds number of 3×10^6 (Ref. 19). Corresponding calculations have been performed with the onset of transition determined, in the absence of experimental information, by the criterion of Ref. 20, and by the onset of laminar separation.

Figures 1 and 2 permit comparison of the measured and calculated values of lift and drag coefficients for the NACA 4412 airfoil. The results for lift coefficient also display the variation with angle of attack that was obtained from the solution of the inviscid-flow equations and that diverges from the measurements with increasing angle. It is also clear that the two calculation methods agree with each other and with experiment up to 8 deg, beyond which the interaction procedure follows

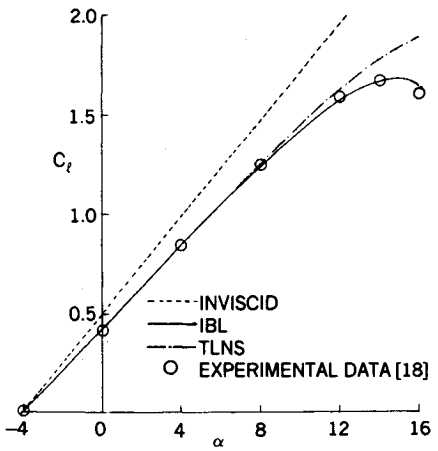

Fig. 1 Variation of lift coefficient with angle of attack for the NACA 4412 airfoil at $R_c = 1.523 \times 10^6$.

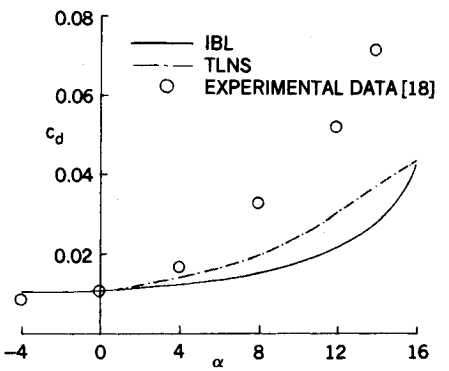

a) $R_c = 1.523 \times 10^6$

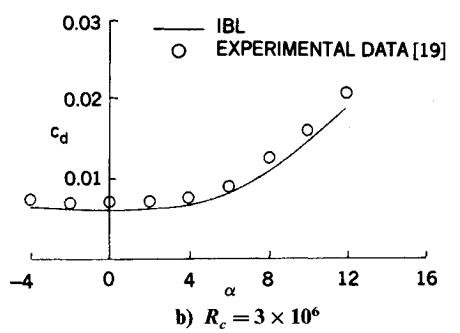

b) $R_c = 3 \times 10^6$

Fig. 2 Variation of total drag coefficient with angle of attack.

the experimental results more closely and represents the expected maximum value at the same angle of attack as the measurements. This aspect of the comparison of the two calculation methods is similar to that reported in Ref. 1 in relation to a NACA 0012 airfoil, with the two calculation methods agreeing with each other up to 14 deg.

The drag coefficients of Fig. 2 are more difficult to appraise since the two experimental distributions differ increasingly with angle of attack and, for example, by a factor of almost two at 12 deg. Experimental differences are common, due to the inaccuracy of integrating the wake profile and to wind-tunnel effects associated with blockage or finite span. The magnitude of the present differences is, however, unusual. The results obtained with the two calculation methods agree with the measurements of Refs. 19 and 21 and are at odds with those of Refs. 17 and 18. The results were obtained by wake integration of the interactive boundary-layer results and by surface integration of the TLNS results since, in the latter case, the far wake was not represented well by the calculations.

Table 1 Comparison of calculated and experimental results for transonic flows

Case 1: NACA 0012 airfoil, $M_\infty = 0.775$, $R_c = 3.5 \times 10^6$			
	IBL	TLNS	Exp (25)
M_∞	0.775	0.775	0.775
α	1 deg	1 deg	1 deg
C_l	0.2066	0.1989	Not available
C_d	0.0121	0.0152	Not available
Case 2: NACA 0012 airfoil, $M_\infty = 0.5$, $R_c = 3 \times 10^6$			
	IBL	TLNS	Exp (26)
M_∞	0.5	0.5	0.5
α	7.86 deg	7.86 deg	7.86 deg
C_l	0.9892	0.9456	Not available
C_d	0.012	0.022	Not available
Case 3: RAE 2822 airfoil, $M_\infty = 0.725$, $R_c = 6.5 \times 10^6$			
	IBL	TLNS	Exp (27)
M_∞	0.729	0.729	0.725
α	2.53 deg	2.59 deg	2.92 deg
C_l	0.743	0.738	0.743
C_d	0.0112	0.0157	0.0127
Case 4: RAE 2822 airfoil, $M_\infty = 0.73$, $R_c = 6.5 \times 10^6$			
	IBL	TLNS	Exp (27)
M_∞	0.734	0.734	0.730
α	2.85 deg	2.79 deg	3.19 deg
C_l	0.803	0.784	0.803
C_d	0.0144	0.0196	0.0168

It is interesting to note that measurments of drag coefficient obtained with NACA 0012 airfoils and described in Refs. 22 and 23 also show discrepancies that increase with angle of attack so that, at 12 deg, the difference was around 15%. The calculations of Ref. 1 revealed similar discrepancies, and it is clear that it is difficult to achieve a high degree of accuracy.

For completeness, Fig. 3 presents distributions of pressure coefficients obtained from the calculation methods at four angles of attack. As can be seen, the distributions agree very closely at 0 and 4 deg angle of attack, and reasonably well at 12 deg. But there are differences in the trailing-edge region, and particularly in the representation of the small region of upper-surface separation that affected the wake. This led, in part, to better representation of the wake by the interaction boundary-layer method. It can also be seen that the pressure peak is very sharp and located almost at the leading edge. The distributions at 16 deg reveal an even more peaky pressure distribution, and the need to specify the onset of transition upstream of the trip can be appreciated.

The discrepancy between the two calculation methods is more evident at 16 deg and involves a large and important difference in the trailing-edge region, where the interactive approach suggests separation some 20% of chord upstream of the trailing edge, and the TLNS method suggests a smaller separation.

The GA(W)-2 airfoil represents a more difficult test, since it is a 13% thick airfoil of supercritical form. Measurements have been reported[24] at a chord Reynolds number of 4.3×10^6 and with transition trips at 7.5% chord on both surfaces. Calculations were performed with both methods and, as before, considered the onset of transition in accord with the experimental configuration, unless the interactive approach indicated a laminar separation bubble. In that case, the onset of transition was

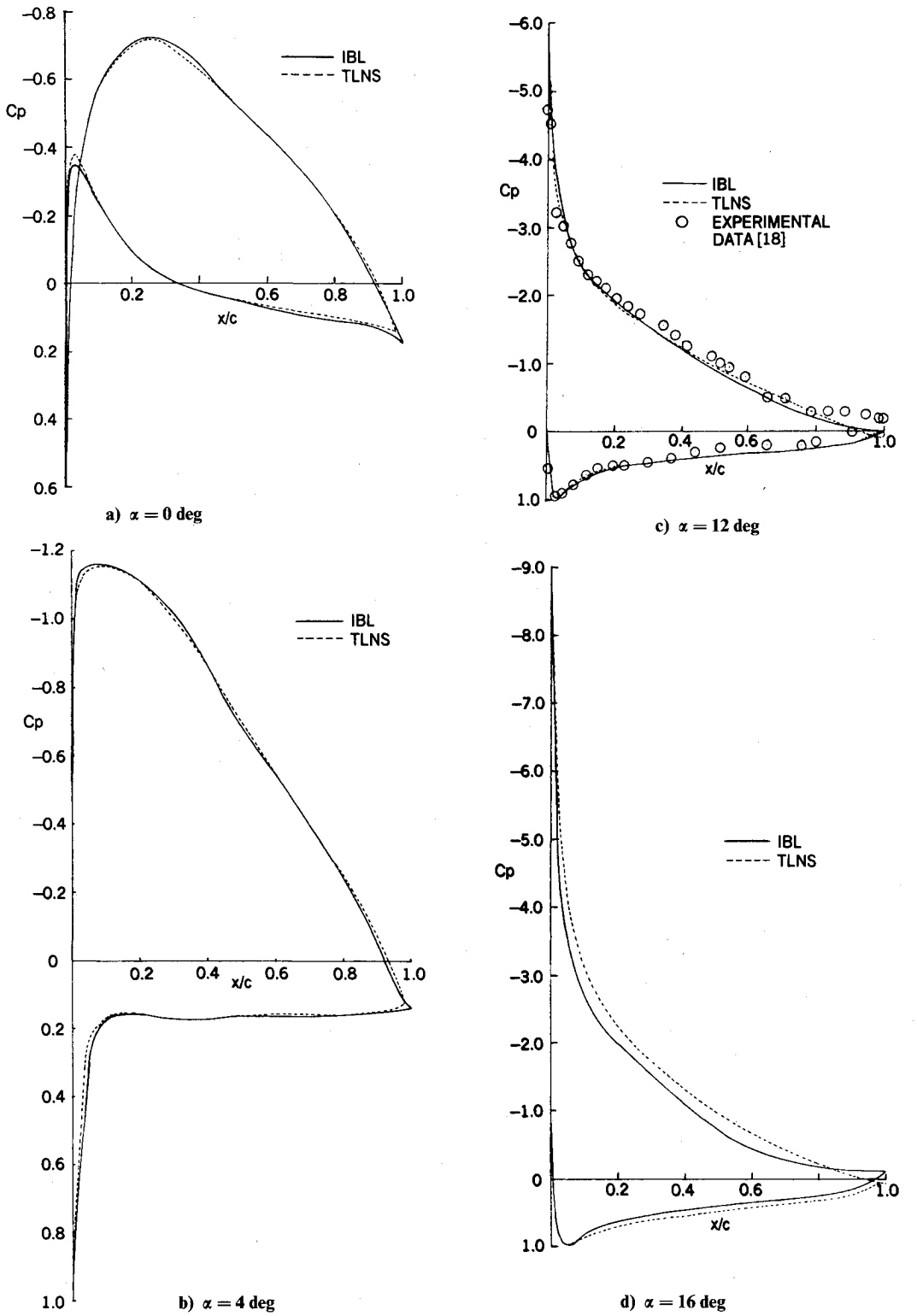

Fig. 3 Comparison of computed pressure distributions at four different angles of attack for the NACA 4412 airfoil at $R_c = 1.523 \times 10^6$.

taken as coincident with the onset of separation. The results shown in Fig. 4 display the variations of lift and drag coefficient with angle of attack.

The deductions that can be made from Fig. 4 are similar to those obtained from Figs. 1 and 2. The two calculation methods represent an improvement over the inviscid-flow calculations in terms of the lift coefficient, and as before, the interactive method provides results in very close agreement with experiment. The interactive method is also able to calculate the drag coefficient satisfactorily at lower angles of attack but with less accuracy as the angle of attack increases so that the difference between measurement and calculation is around 20% at 14 deg. The results of the TLNS method are less satisfactory. A sample of pressure distributions is provided in Fig. 5 and, as before, shows the need for a proper implementation of the TLNS method in the trailing-edge region.

Less-detailed information is available in transonic flow and, as is expected data corresponding to cruise conditions of aircraft are mostly confined to low angles of attack. Thus, measurements have been reported for a NACA 0012 airfoil at 1.00 and at 7.86 deg with corresponding Mach numbers of 0.775 and 0.5[25,26]; and Ref. 27 provides information of the flow

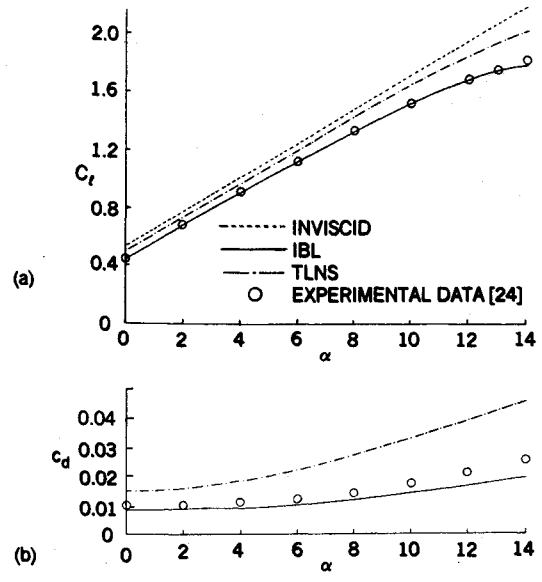

Fig. 4 Variation of lift and drag coefficients for the GA(W)-2 airfoil, $R_c = 4.3 \times 10^6$.

around an RAE 2822 airfoil at 2.92 and 3.19 deg and at Mach number of 0.725 and 0.730, respectively. The pressure distributions for the four cases are presented in Fig. 6, and the calculated lift and drag coefficients are shown in Table 1 together with the experimental values. The calculations for the NACA 0012 airfoil were made by using the experimental Mach numbers and angles of attack, since information regarding wind-tunnel blockage corrections was not available. On the other hand, this information was available for the RAE 2822 airfoil and, as a result, a Mach number higher than 0.004 of that reported in Ref. 27 was used in the calculations. Due to the uncertainty of the angle of attack correction, the experimental lift coefficient was specified in the IBL method. The calculations for the TLNS method were also made under similar conditions, although in this case the angle of attack was input and its value was adjusted until the computed lift coefficient nearly matched the experimental value.

As shown in Fig. 6 and Table 1, the pressure distributions and lift coefficients computed by both procedures agree with each other and with experimental data. As in subsonic flows, however, the calculated drag values by the IBL method are slightly lower than the experimental results, and those computed by the TLNS are consistently higher.

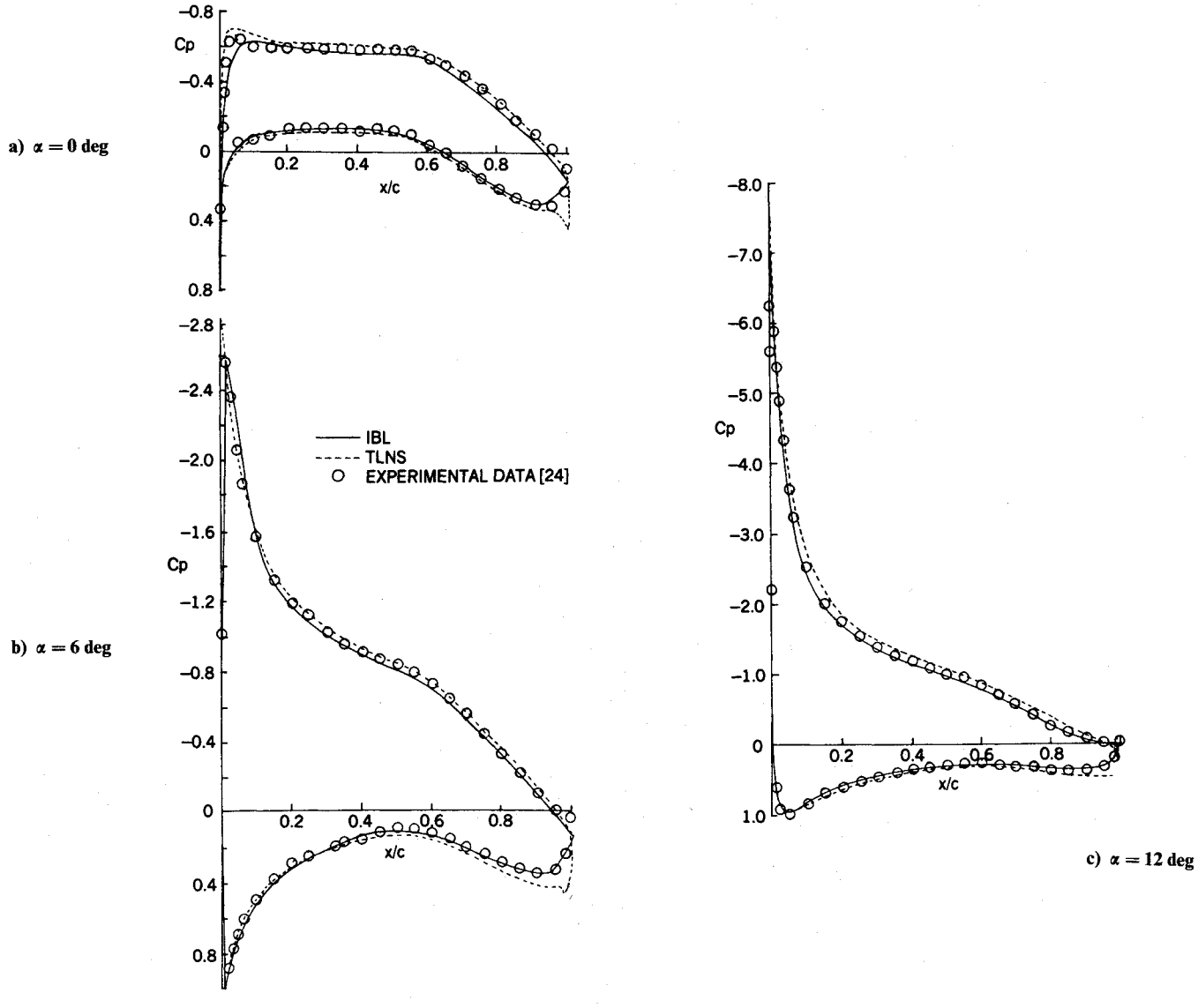

Fig. 5 Comparison of calculated and experimental pressure distributions for the GA(W)-2 airfoil, $R_c = 4.3 \times 10^6$.

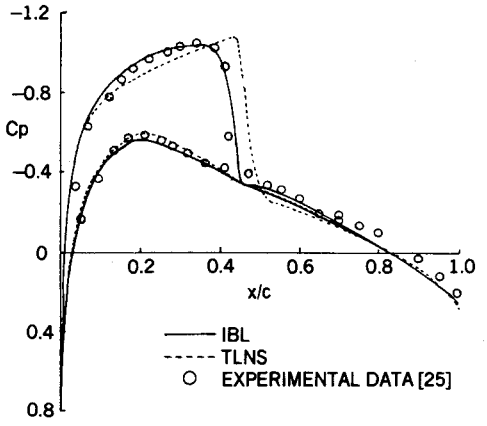

a) NACA 0012 airfoil, $R_c = 3.5 \times 10^6$, $M_\infty = 0.775$, $\alpha = 1$ deg

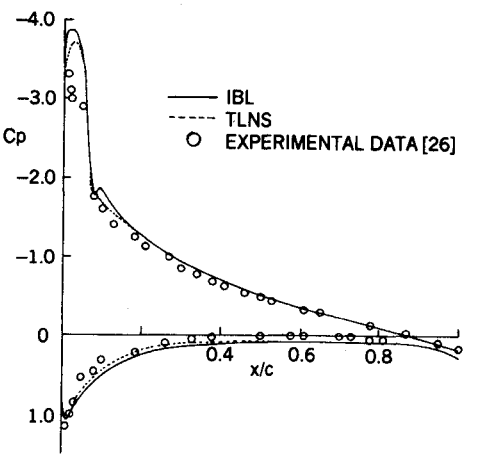

b) NACA 0012 airfoil, $R_c = 3.0 \times 10^6$, $M_\infty = 0.5$, $\alpha = 7.86$ deg

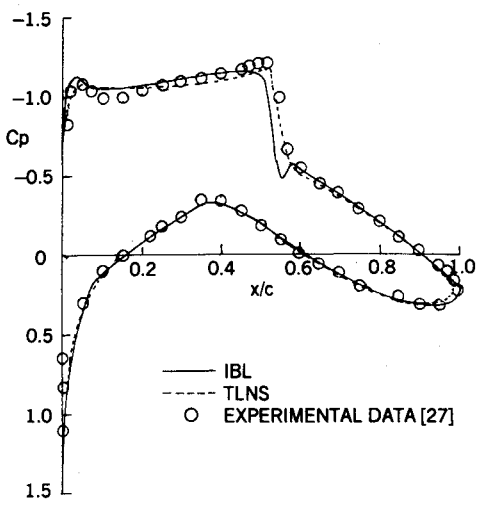

c) RAE 2822 airfoil, $R_c = 6.5 \times 10^6$, $M_\infty = 0.725$, $\alpha = 2.92$ deg

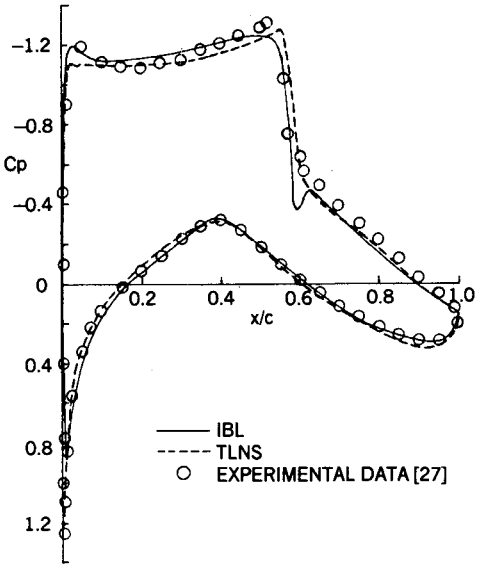

d) RAE 2822 airfoil, $R_c = 6.5 \times 10^6$, $M_\infty = 0.730$, $\alpha = 3.19$ deg

Fig. 6 Comparison of calculated and experimental pressure distributions for transonic flow.

Concluding Remarks

Two separate procedures for computing airfoil characteristics in subsonic and transonic flows are evaluated. The first scheme is based on the solution of the thin-layer Navier-Stokes equations (TLNS), while the second scheme is based on the solution of inviscid- and viscous-flow equations by a special coupling procedure (IBL). Calculations have been performed with essentially the same turbulence model and with identical transition locations. The following conclusions can be drawn from the studies reported in this paper.

1) For subsonic flows, the calculation of the lift coefficient of conventional airfoils at low and moderate angles of attack is obtained with good accuracy by both IBL and TLNS procedures. At flow conditions approaching stall, however, the TLNS results begin to deviate from experimental data and continue to increase with incidence rather than exhibit the "flattening" behavior near $C_{l\max}$. The IBL results, on the other hand, follow the experimental trend well and show good agreement with data, provided that small adjustments are made to the transition location at higher angles of attack.

2) While the results of the IBL procedure are equally satisfactory for airfoils other than conventional ones, those obtained with the TLNS are not. For example, the Navier-Stokes calculations for the GA(W)-2 airfoil show a great deal of sensitivity to the choice of grid distributions near the trailing edge with calculated lift coefficients differing as much as 50% for $\Delta x/c$ increments of 0.001 and 0.01 at the trailing edge. Additional studies are needed to remove this sensitivity and to find the best grid to perform the Navier-Stokes calculations.

3) In general, the drag predictions of the two procedures are different, with the difference becoming more pronounced as the angle of incidence increases. The IBL results seem to be in better agreement with the experiment than the TLNS results, which is somewhat contrary to the conclusion of Ref. 1; however, the data on drag coefficients are not as accurate as those for the lift coefficients. Better data and additional comparisons should be made to reach a more concrete conclusion.

4) For transonic flows, the lift predictions of the two methods are essentially the same. The computed drag coefficients do not agree with experiment as well as the lift coefficients do; the edge in accuracy, however, appears to be with the IBL results.

References

[1]Mehta, U., Chang, K. C., and Cebeci, T., "A Comparison of Interactive Boundary Layer and Thin-Layer Navier-Stokes Procedures," *Numerical and Physical Aspects of Aerodynamic Flows III*, edited by T. Cebeci, Springer-Verlag, New York, 1986, p. 198.

[2]Cebeci, T. and Smith, A. M. O., *Analysis of Turbulent Boundary Layers*, Academic Press, 1974.

[3]Baldwin, B. S. and Lomax, H., "Thin-Layer Approximation and

Algebraic Model for Separated Turbulent Flows," AIAA Paper 78-257. 1978.

[4]Halsey, N. D., "Potential Flow Analysis of Multielement Airfoils Using Conformal Mapping," *AIAA Journal*, Vol. 17, Dec. 1979, p. 1281.

[5]Bauer, F., Garabedian, P. R., Korn, D. G., and Jameson, A., "Supercritical Wing Sections II," *Lecture Notes in Economics and Mathematical Systems*, Springer-Verlag, 1975.

[6]Clark, R. W., "Improved Transonic Airfoil Calculations Using a Partially-Conservative Method," Douglas Aircraft Co. Rept. MDC-J4818, 1986.

[7]Cebeci, T., Chang, K. C., Li, C., and Whitelaw, J. H., "Turbulence Models for Wall Boundary Layers," *AIAA Journal*, Vol. 24, March 1986, pp. 359–360.

[8]Chang, K. C., Bui, M. N., Cebeci, T., and Whitelaw, J. H., "The Calculation of Turbulent Wakes," *AIAA Journal*, Vol. 24, Feb. 1986, pp. 200–201.

[9]Mehta, U., Chang, K. C., and Cebeci, T., "Relative Advantages of Thin-Layer Navier-Stokes and Interactive Boundary-Layer Procedures," NASA TM-86778, 1985.

[10]Cebeci, T., Clark, R. W., Chang, K. C., Halsey, N. D., and Lee, K., "Airfoils with Separation and the Resulting Wakes," *Journal of Fluid Mechanics*, Vol. 163, 1986, p. 323.

[11]Cebeci, T. and Clark, R. W., "An Interactive Approach to Subsonic Flows with Separation," *Numerical and Physical Aspects of Aerodynamic Flows, II*, edited by T. Cebeci, Springer-Verlag, New York, 1984, p. 194.

[12]Cebeci, T., Chen, L. T., and Chang, K. C., "An Interactive Scheme for Three-Dimensional Transonic Flows," *Numerical and Physical Aspects of Aerodynamic Flows, III*, edited by T. Cebeci, Springer-Verlag, New York, 1986, p. 412.

[13]Bradshaw, P., Cebeci, T., and Whitelaw, J. H., *Engineering Calculations of Turbulent Flows*, Academic Press, 1981.

[14]Mehta, U. and Lomax, H., "Reynolds Averaged Navier-Stokes Computations of Transonic Flows—The State-of-the-Art," *Transonic Aerodynamics*, edited by D. Nixon, Progress in Astronautics and Aeronautics, Vol. 81, 1982, p. 297.

[15]Blottner, F. G., "Significance of the Thin-Layer Navier-Stokes Approximation," *Numerical and Physical Aspects of Aerodynamic Flows, III*, edited by T. Cebeci, Springer-Verlag, New York, 1986, p. 184.

[16]Beam, R. and Warming, R. F., "An Implicit Factored Scheme for the Compressible Navier-Stokes Equations," *AIAA Journal*, Vol. 16, March 1978, p. 393.

[17]Wadcock, A. J., "Flying-Hot-Wire Study of Two-Dimensional Turbulent Separation on an NACA 4412 Airfoil at Maximum Lift," Ph.D. Thesis, California Inst. of Technology, Pasadena, CA, 1978.

[18]Coles, D. and Wadcock, A. J., "Flying-Hot-Wire Study of Flow Past an NACA 4412 Airfoil at Maximum Lift," *AIAA Journal*, Vol. 17, Feb. 1979, p. 321.

[19]Pinkerton, R. M., "Calculated and Measured Pressure Distributions Over the Midspan Section of the NACA 4412 Airfoil," NACA Rept. No. 563, 1936.

[20]Michel, R., "Etude de la transition sur les profiles d'aile; establishment d'un critère de determination de la point de transition et calcul de la trainée de la profile incompressible," ONERA Rept. 1/1578A, 1951.

[21]Abbott, J. H. and von Doenhoff, A. E., *Theory of Wing Sections*, Dover, 1959.

[22]Gregory, N. and O'Reilly, C. L., "Low-Speed Aerodynamic Characteristics of NACA 0012 Airfoil Section, Including the Effects of Upper-Surface Roughness Simulating Hoar Frost," NPL Aero Rept. 1308, 1970.

[23]Loftin, L. K., Jr., and Smith, H. A., "Aerodynamics of 15 NACA Airfoil Sections at Seven Reynolds Numbers from 0.7×10^6 to 9×10^6," NACA TN 1945, 1949.

[24]McGhee, R. J., Beasley, W. D., and Somers, D. M., "Low-Speed Aerodynamic Characteristics of a 13-Percent Thick Airfoil Section Designed for General Aviation Application," NASA TM 72697, 1977.

[25]Gregory, N. and Wilby, P. G., "NP-9615 and NACA 0012—Comparison of Aerodynamic Data," Atlantic Research Corporation CP 1261, 1973.

[26]Dvorak, F. A. and Choi, D. H., "Separation Model for Two-Dimensional Airfoils in Transonic Flow," *AIAA Journal*, Vol. 22, Oct. 1984.

[27]Cook, P. H., McDonald, M. A., and Firmin, M. C. P., "Aerofoil RAE 2822—Pressure Distributions and Boundary Layer and Wake Measurements," *Experimental Data Base for Computer Program Assessment*, AGARD-AR-138, 1979.